Intraperitoneal photodynamic therapy for an ovarian cancer ascite model in Fischer 344 rat using hematoporphyrin monomethyl ether

Kun Song,[1] Beihua Kong,[1,6] Li Li,[1,2] Qifeng Yang,[3,4] Yongqing Wei[1] and Xun Qu[5]

[1]Department of Obstetrics and Gynecology, Qilu Hospital, Shandong University, 107 Wenhuaxi Road, Ji'nan, 250012, Shandong, China; [2]Department of Obstetrics and Gynecology, Wakayama Medical University, 811-1 Kimiidera, Wakayama City, Wakayama 641-8509, Japan; [3]The Cancer Institute of New Jersey, Robert Wood Johnson Medical School, 195 Little Albany Street, New Brunswick, New Jersey 08903, USA; [4]Department of General Surgery, Qilu Hospital, Shandong University, 107 Wenhuaxi Road, Ji'nan 250012, Shandong, China; [5]Department of Basic Medicine, Qilu Hospital, Shandong University, 107 Wenhuaxi Road, Ji'nan 250012, Shandong, China

(Received July 8, 2007/Revised August 17, 2007/Accepted August 27, 2007/Online publication September 28, 2007)

With limited treatment options, intraperitoneal spread of ovarian cancer is a common problem leading to high morbidity. Intraperitoneal photodynamic therapy combined with debulking surgery to treat residual disease is an alternative choice for clinicians. Hematoporphyrin monomethyl ether (HMME) is a promising second-generation photosensitizer developed in China. Our study was designed to investigate the phototoxicity of HMME on ovarian cancer. NuTu-19, a cell line derived from adenocarcinoma of Fischer 344 rat, and its allogeneic graft ascites tumor model was used in this study. HMME was confirmed to be localized in cytolysosome, and HMME-based photosensitization induced direct necrosis as well as mitochondria damage. The photocytotoxicity of HMME was both light- and drug dose-dependent and no significant dark cytotoxicity was observed in NuTu-19 cells. With the ascite tumor-bearing Fischer 344 rat model, HMME-based intraperitoneal photodynamic therapy was proved to be useful in improving the prognosis of ovarian cancer. Thus, this study provides evidence that HMME-based photodynamic therapy is an effective adjuvant therapy for ovarian cancer. (*Cancer Sci* 2007; 98: 1959–1964)

Ovarian cancer is the second most common cancer among women and causes more deaths than other cancers of the female reproductive system. An estimated 22 430 new cases and 15 280 deaths are expected in 2007 in the USA.[1] The majority of patients who are diagnosed with ovarian cancer present with advanced-stage disease. Traditional treatment options such as surgery, chemotherapy and radiotherapy have not improved the prognosis significantly during the past decades. The 5-year survival of new ovarian cancer patients remains only 45% in the USA. Hence, an alternative adjuvant treatment method is of high importance besides the conventional therapies for ovarian cancer.

PDT is a novel treatment method used in a wide range of oncological and non-oncological indications, which consists of two simple procedures: the administration of a photosensitizer; and illumination of the tumor to activate the drug. In the prescence of molecular oxygen, the interaction of light with the photosensitizer leads to the formation of reactive oxygen species, primarily singlet oxygen ($^1O_2$), which can react with electron-rich regions of many biomolecules, resulting in oxidative damage to cells and tissues.[2] During PDT, photosensitizer can accumulate preferentially in tumor cells, thereby making PDT-induced damage selective for malignant tissue. Preclinical and clinical trials are showing promise for the treatment of malignancies at multiple sites with minimal normal tissue toxicity. As a minimally invasive technique, PDT can be applied repeatedly at the same site. Furthermore, the use of chemotherapy, ionizing radiation, or surgery does not preclude the use of PDT, making it a promising adjuvant therapy option in tumor patients.[3]

Ovarian cancer tends to spread throughout the abdominal cavity and re-present as disseminated nodules on the surface of the peritonium that remain as regional diseases. In general, PDT can be used as a superficial treatment with a depth of a few millimeters. Thus, intraperitoneal PDT theoretically is an ideal therapy for surface malignancies originating in the abdominopelvic cavity, such as ovarian cancer and other peritoneal carcinomatosis and sarcomatosis. Several preclinical studies have shown the efficiency and toxicity of intraperitoneal PDT to ovarian cancer in animal tumor models using first-generation hematoporphyrin derivative.[4–6] With the development of the photosensitizers, second-generation photosensitizers such as meta-tetrahydroxyphenylchlorin and 5-aminolevulinic acid were also used in intraperitoneal PDT for the treatment of ovarian cancer. Significant delay in tumor regrowth was achieved following meta-tetrahydroxyphenylchlorin-mediated intraperitoneal PDT and a toxicity study has determined the maximum tolerable light dose of ALA-mediated intraperitoneal PDT.[7,8] Hornung *et al*.[9,10] showed that intraperitoneal PDT, as a minimally invasive procedure, could selectively debulk unresectable pelvic ovarian cancer in immunocompetent rats using the pegylated photosensitizer PEG-m-THPC, which was confirmed to be highly targeted to ovarian cancer in a rat model. Several clinical trials using first-generation photosensitizer dihematoporphyrin ether and porfimer sodium showed the therapeutic effects of PDT in treating peritoneal malignancy including ovarian cancer.[11–13] However, the toxicity of the first-generation photosensitizer was notable during the clinical application.[14] More research of intraperitoneal PDT is necessary, using new types of photosensitizers and light sources. HMME, a porphyrin-related photosensitizer that was first developed in China, is a second-generation photosensitizer with lower toxicity, stronger photodynamic effects, higher tumor selectivity, and shorter skin photosensitivity. HMME has been found to be effective in vascular disorders such as port-wine stains and has been approved by the USA's Federal Drug Administration for clinical trials.[15–18] In our previous study, we illustrated the phototoxicity of HMME to SKOV3 ovarian carcinoma cells and its subcutaneous xenograft model in nude mouse.[19] However, ovarian cancer develops in the pelvic cavity and the subcutaneous xenograft model is not consistent with the physiopathologic characteristics of ovarian cancer. Therefore, in this paper we conducted further *in vitro* and *in vivo* studies to

[6]To whom correspondence should be addressed.
E-mail: kongbeihua@yahoo.com.cn

Abbreviations: ALA, 5-aminovulinic acid; CI, confidence interval; DMEM, Dulbecco's modified Eagle's medium; FCS, fetal calf serum; FITC, fluorescein-isothiocyanate; HMME, hematoporphyrin monomethyl ether; MTT, 3-[4,5-dimethylthiazol-2-yl]-2,5-diphenyltetrazolium bromide; PBS, phosphate-buffered saline; PDT, photodynamic therapy; PI, propidium iodide.

doi: 10.1111/j.1349-7006.2007.00628.x

explore the feasibility of HMME-based intraperitoneal PDT for the treatment of ovarian cancer in a Fischer 344 rat ascite tumor model for the first time.

Materials and Methods

Cell lines and culture conditions. Fischer 344 rat-derived epithelial ovarian carcinoma cell line NuTu-19 was a kind gift from Dr Airong Zhang (Second Hospital of Shandong University, Ji'nan, China). NuTu-19 cells were maintained in complete media DMEM (Gibco Life Technologies) with 10% heat-inactivated FCS (Gibco Life Technologies) at 37°C, 5% carbon dioxide, and 100% humidity. All experiments were carried out in exponentially growing cells.

Animals model. Pathogen-free Fischer 344 female rats ($n = 30$, body weight range 100–125 g) were obtained from WeiTong-LiHua, Beijing, China and housed in a pathogen-free animal facility. They were given commercial basal diet and water ad libitum. NuTu-19 cells were harvested with 0.25% trypsin and 0.01% ethylenediaminetetraacetic acid, and washed twice with PBS solution. A total of 10^6 cells was injected intraperitoneally into each rat. The animals were then observed daily and weighed weekly.

Subcellular localization of the photosensitizer. HMME hydrosolvent was provided by FuDan-ZhangJiang Bio-Pharmaceutical Co., Shanghai, China. HMME solution was freshly prepared prior to use by dissolving in PBS at a concentration of 10 mg/mL and kept in the dark at 4°C. Further dilution of HMME was carried out in PBS to reach different concentrations.

Monolayer cells were coincubated in the dark with different concentrations of HMME (5, 30, and 60 μg/mL) and 10 μg/mL mitochondria fluorescent probe (Rhodamine-123; Sigma) or 120 μg/mL cytolysosome fluorescent probe (Lucifer Yellow; Sigma) in Petri dishes at 37°C. Before incubation with the photosensitizer, the samples were washed twice and incubated with Rhodamine-123 for 1 h and with Lucifer Yellow for 15 h. Subcellular staining was observed at various time intervals (0.5, 1, 2, 3, 6, and 12 h) following coincubation. Prior to visualization, excess photosensitizers and probes were washed off and live cells were incubated in fresh medium. Image analysis was accomplished with an Olympus IX81 inverted fluorescence biomicroscope (Olympus, Japan). For detecting the fluorescence of HMME and probes, an excitation filter with wavelengths at 450–480 nm and emission wavelengths > 515 nm was used. Fluorescence images were recorded using a cooled and intensified charge-coupled device camera equipped in the microscope. Image-Pro Plus 6.0 software for Windows (Media Cybernetics, USA) was used to analyze the cell images.

***In vitro* photocytotoxicity assay.** NuTu-19 cells in 200 μL of 10% FCS DMEM medium (1.5×10^4 cells/well) were incubated in 96-well flat-bottomed microtiter plates. When cells were in the exponential growth phase the supernatants were removed and replaced with 200 μL fresh FCS-free medium containing different concentrations of HMME (0–20 μg/mL) for 3 h. The medium containing the drug was then aspirated and the cells were rinsed with PBS. Before laser irradiation, another 200 μL DMEM was added into each well. The laser source was a pulsed dye laser (Quantel Datachrom 5000; Quantel, France) operated at a frequency of 10 Hz. Irradiation was carried out at different light doses (0–6 J/cm^2) at 620 nm with an output power 160 mW. The total power intensity was measured using an EPM2000 power meter (Molectron Detector). Following this treatment, the medium was replaced by 10% FCS DMEM medium and the cells were incubated for another 24 h. Photosensitizer-mediated cytotoxicity was determined by the tetrazolium chlorimetric reduction assay (MTT assay), which measures the mitochondrial dehydrogenase activity of surviving cells, as described previously.[20,21] Briefly, the cells with media only served as a positive control and 200 μL of the medium alone without cells and reagent was used as a negative control. Following photodynamic treatment of the cells in microtiter plates as mentioned above, 20 μL of the MTT dye (5 mg/mL) was added into each well. The unreactive supernatants in the well were carefully aspirated and replaced with 100 μL of isopropanol supplemented with 0.05 M HCl to solubilize the reactive dye. The absorbance (A) values of each well at 540 nm were read using an automatic multiwell spectrophotometer (Bio-Rad, Richmond, CA). The negative control well was used for zeroing absorbance. The percentage of survival was calculated using the background-corrected absorbance as follows:

$$\text{Survival rate} = A \text{ of experimental well}/A \text{ of positive control well} \times 100\%$$

Experiments were carried out at least three times with representative data presented.

Mitochondria damage detection. NuTu-19 cells were incubated in 12-well flat-bottomed microtiter plates. Three hours after HMME was added, the cells received photodynamic treatment (HMME 5 μg/mL, light dose 5 J/cm^2) as described above. The cell samples were rinsed with fresh medium and stained with the Mitochondrial Apoptosis Detection Kit (BioVision) according to the manufacturer's instructions at 4 and 8 h after irradiation. All images were then captured using the Olympus IX81 fluorescent microscope to assess the site of mitochondrial damage. Blank cells without any treatment served as controls.

Apoptosis or necrosis detection. Apoptosis or necrosis detection post-PDT were determined by flow cytometer using the Annexin V–FITC Apoptosis Kit (BioVision). Briefly, approximately 1×10^6 NuTu-19 cells that had received photodynamic treatment (HMME 5 μg/mL, light dose 5 J/cm^2, 3 h after incubation) were gently scraped and washed twice with cold PBS at 4 h and 8 h following photodynamic treatment. Cells were resuspended with 100 μL annexin-V binding buffer then incubated with 10 μL annexin-V for 15 min at room temperature in the dark. Then 400 μL binding buffer containing 5 μL PI was added to the cells and incubated on ice for 15 min. The cells were sampled with a FacsCalibur flow cytometer (Becton Dickinson) within 1 h. A total of 1×10^4 cells were analyzed in each sample. Data analysis was carried out with CELLQuest software (Becton Dickinson). The results were interpreted as follows: cells that were annexin V(–)/PI(–) (lower left quadrant) were considered as living cells; annexin V(+)/PI(–) cells (lower right quadrant) as apoptotic cells, annexin V(+)/PI(+) (upper right quadrant) as necrotic cells; and annexin V(–)/PI(+) (upper left quadrant) may be bare nuclei, cells in late necrosis, or cellular debris.

PDT *in vivo*. Six weeks following 1×10^6 cells innoculation, the tumor-bearing Fischer 344 rats were divided randomly into three groups. The control groups included animals that received cytoreductive surgery (group A) and those that received cytoreductive surgery followed by laser illumination (group B). In the treatment group (group C), HMME at a dose of 10 mg/kg body weight was injected intraperitoneally. Three hours after injection, cytoreductive surgery was carried out, followed by a laser delivered to the surface of the abdominal cavity. All animals were anesthetized by pentobarbital sodium (40 mg/kg) given intraperitoneally before surgery. A heating device was used to keep body temperature stable throughout the treatment until the animal was woken up. All macroscopic niduses were removed and omentectomy was carried out during the operation. The total energy of the laser delivered to each rat was 50 J/cm^2 with an ouput power of 160 mW. The laser source was a pulsed dye laser operated at a frequency of 10 Hz. To keep the laser output power stable, the room temperature was kept at 25°C throughout the experiment. The beam of laser was exported horizontally from the outlet then delivered through a refracting prism system to vertically cover the rat's peritoneal cavity. In order to avoid

doi: 10.1111/j.1349-7006.2007.00628.x

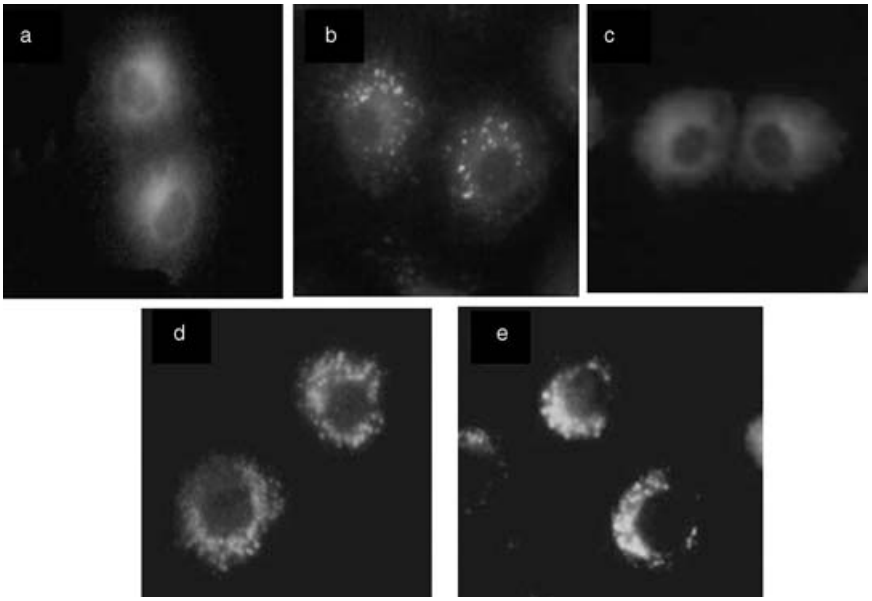

Fig. 1. Subcellular localization of hematoporphyrin monomethyl ether (HMME) in NuTu-19 cells derived from adenocarcinoma of Fischer 344 rat. Fluorescence images of the cells double-stained with HMME and mitochondria fluorescent probe (Rhodamine-123; Sigma) or cytolysosome fluorescent probe (Lucifer Yellow; Sigma) are shown. Cells were observed at various time intervals (0.5, 1, 2, 3, 6, and 12 h) following coincubation of HMME and Rhodamine-123 or Lucifer Yellow. (a) HMME + Rhodamine-123; (b) HMME + Lucifer Yellow; (c) HMME alone; (d) Rhodamine-123 alone; (e) Lucifer Yellow alone. All photos were taken 3 h after incubation.

the loss of laser energy, light fiber was not used in our study. The laser power was measured with a power meter and the average irradiation time was 20 min for each rat. During PDT 0.9% warm sodium chloride solution was dripped into the peritoneal cavity continuously to avoid evaporation of body fluid and damage to organs caused by thermal effect. The tumor tissues dissected during the surgery were placed immediately in 10% formalin followed by routine processing of histolotgical study to confirm the development of cancer. The peritoneal cavity was sutured with sterile surgical wire. The entire procedure was carried out under sterile conditions. After treatment the animals were observed daily and followed up for 2 months. Survival studies were initiated in all three groups following treatment. The end point was defined as rat death due to ovarian cancer, with evidence of cachexia such as a large number of ascites, anemia, and serious emaciation. Survival analysis was evaluated using Kaplan–Meier survival analysis. Survival curves were drawn and the differences in survival times among three groups were tested for significance.

Statistical analysis. The statistical analysis was carried out using SPSS 13.0 for Windows (SPSS). Differences between groups were analyzed by two-way ANOVA tests and the Student–Newman–Keuls' Q-test for significance. Survival studies was evaluated using Kaplan–Meier survival analysis. $P < 0.05$ indicates statistical significance.

Results

Intracellular localization by fluorescence microscopy. Distinctive intracellular localization was achieved using the special fluorescence probes in living NuTu-19 cells. Fig. 1 shows typical fluorescence images of the double-stained cells with HMME and a subcellular organelles probe (Rhodamine-123 or Lucifer Yellow). After incubation with HMME alone, diffuse red fluorescence was observed in the cytoplasm. No HMME fluorescence was observed in the nucleus (Fig. 1c). As shown in Fig. 1(d,e) the mitochondria probe and the cytolysosome fluorescent probe emitted green fluorescent spots in the cytoplasm. The combined images of both HMME and probes should present yellow fluorescent spots indicating an overlap of HMME (red) and probes (green). In cells treated with HMME and Lucifer Yellow, there were clear yellow spots in the cytoplasm 0.5 h following incubation when 30 μg/mL and 60 μg/mL HMME was given (Fig. 1b). However, the yellow spots appeared 1 h later when a lower HMME dose (5 μg/mL) was given. The common yellow spots did not appear in HMME and Rhodamine-123 double-stained cells in despite of the different drug doses (5, 30, and 60 μg/mL) and incubation times (0.5, 1, 2, 3, 6, and 12 h), indicating that no HMME was confined to mitochondria (Fig. 1a). The HMME subcellular localization pattern was identical for various drug concentrations and incubation intervals. It was apparent that HMME was localized at the cytolysosome which seemed to be the target of HMME-based PDT.

***In vitro* phototoxicity.** MTT assay showed that there was no significant difference in the survival rate of cells exposed to light alone ($P > 0.05$) or HMME alone ($P > 0.05$) compared to blank controls (neither light nor HMME). HMME alone or laser alone showed no cytotoxicity to NuTu-19 cells, which was important because it indicated that no dark toxicity existed concerning HMME. When HMME combined with laser illumination, the photocytotoxicity were both drug dose- and light dose-dependent. The survival rate of cells was significantly decreased with increasing light dose (2–6 J/cm^2, $P = 0.004$). The same difference was observed with an increasing HMME dose (1.25–20 μg/mL, $P = 0.001$). NuTu-19 cells seemed very sensitive to HMME-based PDT. When the HMME dose reached 20 μg/mL, all cells were killed even in a lower laser dose (2 J/cm^2). The survival rate curve is shown in Fig. 2.

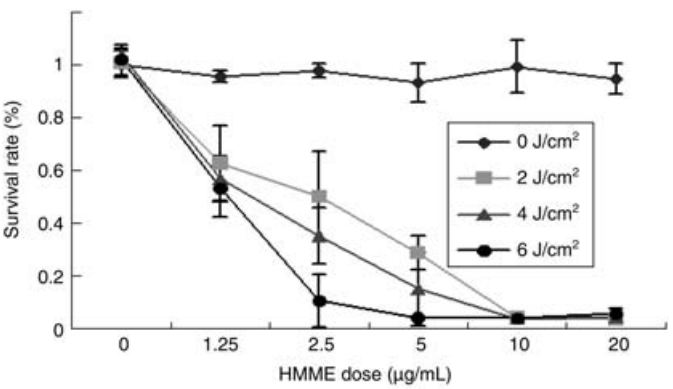

Fig. 2. Photocytotoxity of hematoporphyrin monomethyl ether (HMME) to NuTu-19 cells derived from adenocarcinoma of Fischer 344 rat. Shown are the cell survival rates at 24 h after photodynamic treatment with different concentrations of HMME (0–20 μg/mL) and different light doses (0–6 J/cm^2).

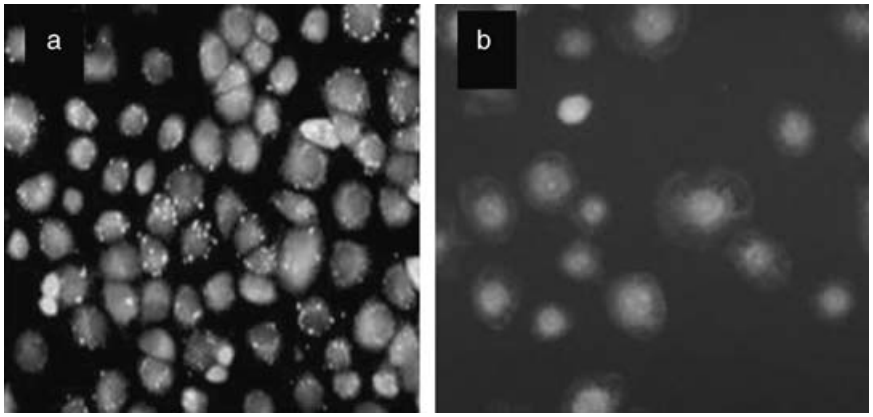

Fig. 3. Mitochondria damage in NuTu-19 cells, derived from adenocarcinoma of Fischer 344 rat, following hematoporphyrin monomethyl ether photodynamic treatment. (a) Orange fluorescent spots in control cells indicate the intact mitochondria. (b) Mitochondria fluorescent spots disappeared completely and there were only diffused weaker green fluorescent spots in the cytoplasm, indicating the mitochondria damage.

Mitochondria damage and death mode detection. Fig. 3(a) shows orange fluorescent spots with green background in the cytoplasm of control NuTu-19 cells (without any treatment), indicating the intact mitochondria. Mitochondria fluorescent spots disappeared completely and there was only weaker diffused green fluorescence in the cytoplasm following PDT, which indicated mitochondria damage, as shown in Fig. 3(b). The same results were observed 4 and 8 h following photodynamic treatment.

At 4 and 8 h following PDT, dual staining of cells with Annexin V\PI and analysis using flow cytometry were used to distinguish apoptotic from necrotic cells. Flow cytometry dot plots of the simultaneous binding of Annexin V–FITC and PI uptake by cells are shown in Fig. 4. The dead cells were mainly characterized as Annexin V(+)/PI(+), representing necrosis. Therefore, HMME-based PDT induced direct necrosis rather than apoptosis in NuTu-19 cells.

Effectiveness of HMME-based intraperitoneal PDT on ascite tumor model. NuTu-19 cells grew progressively in the abdominal cavity in a manner typical of human ovarian epithelial carcinomas. All animals in the experiment developed cancer in the peritoneal cavity following injection with 10^6 cells, represented by numerous serosal nodules (peritoneum, omentum, diaphragm, and bowel), omentum contraction, and malignant bloody ascites. Pathohistology results confirmed the existence of adenocarcinoma tissue.

At the end of the study, the survival rate of the treatment group (group C) was 33.3%, with a median follow-up time of 45 days (95% CI, 1.17–88.83 days). In the control groups, the median follow-up was 15 days (95% CI, 6.68–23.32 days) and 19 days (95% CI, 13.16–24.84 days) in groups A and B, respectively. There was no statistically significant difference on the survival time between the two control groups ($P = 0.788$). No animals survived in control groups when the study was closed. PDT could prolong the survival time significantly compared to the controls ($P = 0.008$). The Kaplan–Meier survival curves of the three groups are shown in Fig. 5.

Discussion

In the past half century, with the development of new types of photosensitizers and new light delivery systems, PDT has attracted people's interest as a unique treatment method.[22] PDT offers an alternative option in cancer management and has been used for localized superficial or endoluminal malignant and premalignant conditions. The poor prognosis of advanced ovarian cancer and recent developments in photomedicine have generated considerable interest in PDT for this disease. Much work has been done and clinical trials show promising results concerning this new approach. However, its use remains

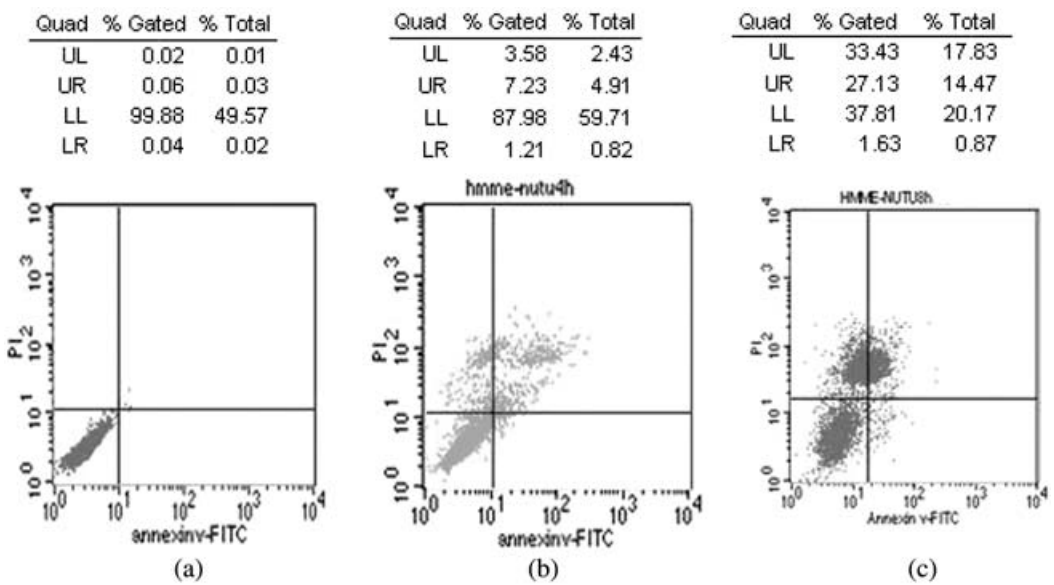

Fig. 4. Cell death mode induced by hematoporphyrin monomethyl ether-based photodynamic treatment (PDT). Flow cytometry analysis of NuTu-19 cancer cells, derived from adenocarcinoma of Fischer 344 rat. with Annexin V/propidium iodide (PI) double staining after PDT. (a) Controls; (b) 4 h after PDT; (c) 8 h after PDT. UL (upper left quadrant): Annexin V(–)\PI(+), cell fragment; UR (upper right quadrant): Annexin V(+)\PI(+), necrosis cells; LL (lower left quadrant): Annexin V(–)\PI(–), survival cells; LR (lower right quadrant): Annexin V(+)\PI(–), apoptotic cells.

doi: 10.1111/j.1349-7006.2007.00628.x

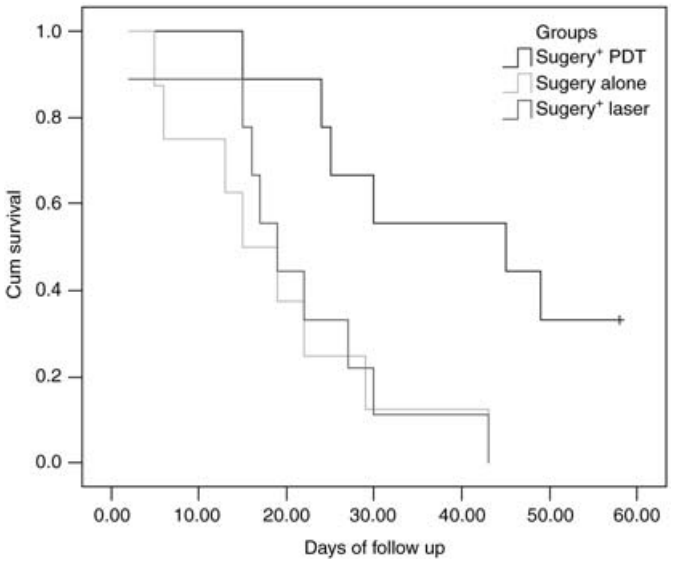

Fig. 5. Kaplan–Meier survival curves for tumor-bearing Fischer 344 rats. Treatment groups (n = 9) included animals that received cytoreductive surgery and intraperitoneal photodynamic treatment (hematoporphyrin monomethyl ether 10 mg/kg, laser 50 J/cm^2). Control groups included animals that received cytoreductive surgery alone (n = 8) or cytoreductive surgery followed by laser illumination (50 J/cm^2) without photosensitizer (n = 9).

marginal because PDT has no clear established advantages over alternatives such as chemotherapy and radiotherapy. Before its wide application in the clinic, more evidence is needed concerning the effect of PDT on ovarian cancer. In the current study, we provided evidence of HMME-based PDT efficiency in NuTu-19 cells and its allogeneic graft ascites tumor model, a reliable, immunocompetent epithelial ovarian cancer animal tumor model that developed in a manner typical for human ovarian epithelial carcinomas.[23]

The effect of PDT depends on the formation of reactive oxygen species such as singlet oxygen ($^1O_2$). Owing to the short intracellular lifetime of the biochemically active singlet oxygen species, the diffusion range of $^1O_2$ is limited to approximately 45 nm in cellular media.[24] Because the diameter of human cells ranges from approximately 10 to 100 μm, the site of the primary generation of $^1O_2$, where the photosensitizer locates, consequently determines which subcellular structures might be attacked. Therefore, it is not surprising that the type of the response triggered by activation of the photosensitizers depends on their intracellular localization. In this study a mitochondria probe and a cytolysosome probe combined with HMME were used to stain the cells to find the subcellular location of HMME. The images in fluorescence microscopy revealed that HMME was localized in cytolysosome, which indicated the intracellular targets of HMME PDT. There was no accumulated fluorescence of HMME in mitochondria. Increasing evidence has shown that mitochondrial damage is a major cause of phototoxicity.[25,26] Observations of mitochondrial damage after photosensitization was interesting because mitochondrial depolarization was an early step leading to cell death. Release of cytochrome c from mitochondria can activate caspases that trigger death signals from upstream events.[27,28] However, Kessel *et al*.[29] found that photosensitizers localized to non-mitochondrial organelles also caused depolarization of mitochondria. This could explain why mitochondria were damaged completely in NuTu-19 cells following HMME-based photosensitization, even though HMME fluorescence was not found in mitochondria in our study. We found that necrosis, instead of apoptosis, occurred in NuTu-19 cells treated by HMME-based photosensitization. PDT can induce cell death through necrosis and/or apoptosis and the type of cell death depends on the photosensitizer's physicochemical properties, the illumination conditions, the type of cells involved, and PDT dose.[30,31] Ding *et al*.[15] reported apoptosis induced by HMME PDT in cervical cancer cell line HeLa, which is not consistent with our results. These findings suggest that the cell type might be the determining factor in the death mode induced by HMME-based PDT. In addition, the cytolysosome, where HMME was localized in NuTu-19 cells, could release lytic enzymes following photosensitization then induce necrosis directly. In our study we used pulsed laser instead of continuous laser, which is probably another influential factor.

PDT *iv vitro* and *in vivo* comfirmed the phototoxicity of HMME to ovarian cancer. HMME-based phototoxicity was dose-dependent *in vitro*. HMME alone had no influence on NuTu-19 cells, indicating the absence of dark toxity, one of the essential properties for an ideal photosensitizer. In Fischer 344 rats bearing ascite tumors, HMME-based intraperitoneal PDT followed by cytoreductive sugery could prolong survival significantly compared to the controls. Intraperitoneal PDT-related toxicity, such as bowel perforation, did not appear in our study. This might be attributed to the less penetrating 620 nm wavelength and the lower light dose (50 J/cm^2) delivered to the animals. The choice of light source and PDT dose are of high importance in the use of intraperitoneal PDT. In clinical applications, shorter wavelength light might be helpful in avoiding complications such as intestinal perforation.

To conclude, HMME was localized in the cytolysosome and HMME-based photosensitization induced direct necrosis instead of apoptosis in NuTu-19 cells. Our *in vitro* and *in vivo* studies proved that HMME-based PDT is effective for ovarian cancer treatment. However, more evidence-based medicine research, such as prospective randomized clinical trials with large sample sizes, is warranted before it is used in clinical practice.

Acknowledgments

This work was supported by grants from the National Natural Science Foundation of China (No. 30571953) to B.K. and the TaiShan Scholar Foundation of Shandong Province, China.

References

1 American Cancer Society. *Cancer Facts and Figures 2007*. Atlanta, GA: American Cancer Society, 2007.
2 Ochsner M. Photophysical and photobiological processes in the photodynamic therapy of tumours. *J Photochem Photobiol B* 1997; **39**: 1–18.
3 Triesscheijn M, Baas P, Schellens JH *et al*. Photodynamic therapy in oncology. *Oncologist* 2006; **11**: 1034–44.
4 Tochner Z, Mitchell JB, Smith P *et al*. Photodynamic therapy of ascites tumours within the peritoneal cavity. *Br J Cancer* 1986; **53**: 733–6.
5 Tochner Z, Mitchell JB, Harrington FS *et al*. Treatment of murine intraperitoneal ovarian ascitic tumor with hematoporphyrin derivative and laser light. *Cancer Res* 1985; **45**: 2983–7.
6 Tochner Z, Mitchell JB, Hoekstra HJ *et al*. Photodynamic therapy of the canine peritoneum: normal tissue response to intraperitoneal and intravenous photofrin followed by 630 nm light. *Lasers Surg Med* 1991; **11**: 158–64.
7 Veenhuizen RB, Ruevekamp MC, Oppelaar H *et al*. Foscan-mediated photodynamic therapy for a peritoneal-cancer model: drug distribution and efficacy studies. *Int J Cancer* 1997; **73**: 230–5.
8 Major AL, Rose GS, Svaasand LO *et al*. Intraperitoneal photodynamic therapy in the Fischer 344 rat using 5-aminolevulinic acid and violet laser light: a toxicity study. *J Photochem Photobiol B* 2002; **66**: 107–14.
9 Hornung R, Fehr MK, Monti-Frayne J *et al*. Minimally-invasive debulking of ovarian cancer in the rat pelvis by means of photodynamic therapy using the pegylated photosensitizer PEG-m-THPC. *Br J Cancer* 1999; **81**: 631–7.
10 Hornung R, Fehr MK, Monti-Frayne J *et al*. Highly selective targeting of ovarian cancer with the photosensitizer PEG-m-THPC in a rat model. *Photochem Photobiol* 1999; **70**: 624–9.

11 DeLaney TF, Sindelar WF, Tochner Z *et al*. Phase I study of debulking surgery and photodynamic therapy for disseminated intraperitoneal tumors. *Int J Radiat Oncol Biol Phys* 1993; **25**: 445–57.
12 Hendren SK, Hahn SM, Spitz FR *et al*. Phase II trial of debulking surgery and photodynamic therapy for disseminated intraperitoneal tumors. *Ann Surg Oncol* 2000; **8**: 65–71.
13 Hahn SM, Fraker DL, Mick R *et al*. A phase II trial of intraperitoneal photodynamic therapy for patients with peritoneal carcinomatosis and sarcomatosis. *Clin Cancer Res* 2006; **12**: 2517–25.
14 Canter RJ, Mick R, Kesmodel SB. Intraperitoneal photodynamic therapy causes a capillary-leak syndrome. *Ann Surg Oncol* 2003; **10**: 514–24.
15 Ding X, Xu Q, Liu F *et al*. Hematoporphyrin monomethyl ether photodynamic damage on HeLa cells by means of reactive oxygen species production and cytosolic free calcium concentration elevation. *Cancer Lett* 2004; **216**: 43–54.
16 Gu Y, Huang NY, Liang J *et al*. Clinical study of 1949 cases of port wine stains treated with vascular photodynamic therapy (Gu's PDT). *Ann Dermatol Venereol* 2007; **134**: 241–4. (In French.)
17 Zheng H. Photodynamic therapy in China: over 25 years of unique clinical experience. Part one – history and domestic photosensitizers. *Photodiag Photodynamic Ther* 2006; **3**: 3–10.
18 Xu D-Y. Research and development of photodynamic therapy photosensitizers in China. *Photodiag Photodynamic Ther* 2007; **4**: 13–25.
19 Song K, Kong B, Qu X *et al*. Phototoxicity of hemoporfin to ovarian cancer. *Biochem Biophys Res Commun* 2005; **337**: 127–32.
20 Kong B, Wang W, Liu C *et al*. Efficacy of lentivirus-mediated and MUC1 antibody-targeted VP22-TK/GCV suicide gene therapy for ovarian cancer. *In Vivo* 2003; **17**: 153–6.
21 Yang Q, Shan L, Yoshimura G *et al*. 5-aza-2′-deoxycytidine induces retinoic acid receptor beta 2 demethylation, cell cycle arrest and growth inhibition in breast carcinoma cells. *Anticancer Res* 2002; **22**: 2753–6.
22 Brown SB, Brown EA, Walker I. The present and future role of photodynamic therapy in cancer treatment. *Lancet Oncol* 2004; **5**: 497–508.
23 Rose GS, Tocco LM, Granger GA *et al*. Development and characterization of a clinically useful animal model of epithelial ovarian cancer in the Fischer 344 rat. *Am J Obstet Gynecol* 1996; **175**: 593–9.
24 Sobolev AS, Jans DA, Rosenkranz AA. Targeted intracellular delivery of photosensitizers. *Prog Biophysics Mol Biol* 2000; **73**: 51–90.
25 Morgan J, Oseroff AR. Mitochondria-based photodynamic anti-cancer therapy. *Advanced Drug Delivery Rev* 2001; **49**: 71–86.
26 Hilf R. Mitochondria are targets of photodynamic therapy. *J Bioenerg Biomembr* 2007; **39**: 85–9.
27 Yang J, Liu X, Bhalla K *et al*. Prevention of apoptosis by Bcl-2: release of cytochrome c from mitochondria blocked. *Science* 1997; **275**: 1129–32.
28 Kluck RM, Bossy-Wetzel E, Green DR *et al*. The release of cytochrome c from mitochondria: a primary site for Bcl-2 regulation of apoptosis. *Science* 1997; **275**: 1132–6.
29 Kessel D, Luo Y, Deng Y *et al*. The role of subcellular localization in initiation of apoptosis by photodynamic therapy. *Photochem Photobiol* 1997; **65**: 422–6.
30 Almeida RD, Manadas BJ, Carvalho AP, Duarte CP. Intracellular signaling mechanisms in photodynamic therapy. *Biochim Biophys Acta* 2004; **1704**: 59–86.
31 Wyld L, Reed MW, Brown NJ. Differential cell death response to photodynamic therapy is dependent on dose and cell type. *Br J Cancer* 2001; **84**: 1384–6.

doi: 10.1111/j.1349-7006.2007.00628.x